Scanning Electron Microscopy

Volume 3
Number 1 *3rd Pfefferkorn Conference*

Article 12

1984

Computer Programs for Analyzing Certain Classes of 3-D Electrostatic Fields with Two Planes of Symmetry

Norm Franzen
Tektronix Inc.

Electron Optical Systems (pp. 115-126)
SEM Inc., AMF O'Hare (Chicago), IL 60666-0507, U.S.A.

0-931288-34-7/84$1.00+.05

COMPUTER PROGRAMS FOR ANALYZING CERTAIN CLASSES OF 3-D ELECTROSTATIC FIELDS WITH TWO PLANES OF SYMMETRY

Norm Franzen

Tektronix, Inc.
P.O. Box 500
Beaverton, OR 97077
Phone No. (503) 627-5136

Abstract

At Tektronix, two classes of non-rotationally symmetric electrostatic lenses which lead to significant three-dimensional-field problems are currently under investigation. Extensive interactive computer programs have been developed to study these lens structures.

The first class is referred to as Klemperer *lipped* lenses; the accelerating quadrupole being the most important. Klemperer lenses are formed from shaped concentric cylindrical electrodes and employ two or three independent voltages. These lenses are predominantly of quadrupole type, but possess higher multipoles to correct for geometry distortion.

The second class of lenses, referred to as *wafer-lenses,* consists of lenses formed from spaced sequences of metal wafer electrodes with varying apertures and two planes of symmetry. Typical lenses formed in this manner include quadrupoles, octopoles, slot-lenses, stigmators and solid quadrupoles with exit field shaping.

The primary method of calculation used here is three-dimensional relaxation in either a rectangular or cylindrical coordinate mesh representing one quadrant of the field. The three-dimensional relaxation is followed by multipole decomposition of the core field using Fast Fourier Transforms (FFTs). Numerous graphical methods are used for program diagnostics and to display lens distortions. The electrodes are described by simple shape parameters and the computer program does the complete analysis of the boundary conditions. Program setup time for a complex lens can be less than one half hour. Large fields can be segmented if necessary.

Key Words: Electron Optics, electrostatic quadrupoles relaxation methods, meshless scan expansion, Klemperer lenses, wafer lenses, Fourier-Bessel expansion, Electron gun.

Introduction

With ever greater frequency, designers of electron optical systems are employing electrostatic and magnetostatic fields which cannot be reduced to two-dimensional field problems. Most deflection systems are of this type.[13,15] The newer in-line gun systems for color raster displays employ non-rotationally symmetric optics.[6,11] Beginning with Martin and Deschamps,[12] designers of electron guns for oscilloscopes, have begun to exploit the advantages of quadrupole optics.[2,3,5,8,14] In each of the problem areas covered in the referenced material, field calculations are confronted that stress the capabilities of modern high-speed computers. Not being reducible to two dimensions or amenable to classical analysis, such three-dimensional problems would not have been attempted at all just a few short years ago.

The most frequently used method for two-dimensional problems has been the finite difference method (FDM) or relaxation technique. To most researchers this method did not seem feasible in three dimensions since as many as 10,000 to 100,000 mesh nodes might be required to represent the field. However in 1977 Odenthal,[14], developed a three-dimensional program using relaxation methods to study the *Box-lens.* Roughly 30,000 mesh nodes were used and the relaxation process converged in 90 CPU seconds on a CYBER 73 system. The success of the method rested in the fact that the electrodes were situated in coordinate planes.

This article will show that there are other quite large classes of non-rotationally symmetric lens structures that can be analyzed by finite difference methods. In fact the ease of use and setup procedure for the study of these structures is vastly more simple than for most of the newer methods. The setup time for some rather complex lens configurations discussed below can be measured in minutes rather than hours or days.

The FDM techniques employed at Tektronix cannot be readily adapted to the treatment of misaligned structures, however the method referred to as the charge density or *Boundary Element Method (BEM)* seems to be most suited for such calculations. A. Wexler and his students,[10,18], have combined this method with techniques for smooth modeling of surfaces. This approach has the virtue of having to store only the sources on two-dimensional surfaces as well as yielding efficient means to perform the required surface integrals. In Wexler's approach the concept of *surface*

spline or *Coons-patch,*[1], is employed to represent the subelectrodes and interconnect them in a smooth fashion. The charge is not assumed to be constant over such patches but takes a form convenient for performing the surface integrals by Gaussian quadrature. The accidental singularity when $|r - r'| = 0$ in $\int \varrho\,(r')/|r - r'|da$ is given special attention. Since the surfaces and integrals are setup in parametric form, the electrodes can be tilted in space by simple transformations without complications. The charge distribution is determined by a variational principle which is a form of the *Method of Moments* as discussed by R. Harrington.[4] As is the case for the *Finite Element Method* (FEM), the Boundary Element Method requires the inversion of a *large matrix.* Usually the number of subelectrodes is much less for the BEM than the number of elements required for the FEM approach. Also the *elements* are confined to surfaces so the subdivision process is much simpler.

Since it is our primary purpose to demonstrate the utility of the Finite Difference Method (FDM) in certain significant classes of electrostatic field problems with two planes of symmetry, the class of structures called Klemperer lenses is briefly reviewed in the following paragraph.

Klemperer Lenses of Type I & II

In the second edition of his textbook *Electron Optics,*[9], published in 1953, Klemperer proposed two quadrupole type accelerating lenses as shown in figures 1a and 1b. Both lenses have been called MSE lenses, an abbreviation for *meshless scan expansion.* MSE lenses are being used to displace the dome-mesh scan expansion lens commonly employed in electron guns used in high performance oscilloscopes. The Type I lens is also called the *In-line* lens for obvious reasons. The Type II lens is referred to as the *Low-Voltage Profile lens,* or LVMSE. In each case the entrant electrode on the left is operated at gun potential, say 2 kV, and the exit electrode is at screen potential, say 10–20 kV. Both Type I and Type II lenses have played an important role in the development of the quadrupole gun design displayed in figures 2a and 2b.* These figures show the action of the four quadrupoles (Q1,Q2,Q3, and Q4) in the formation of the beam, and the development of the scan from the deflection system. Quadrupoles Q1 and Q2 are adjusted to regain focus with change in drive, while Q3 and Q4 operate in a static mode and together constitute the scan-expansion and accelerating system. Further details of the operation of the gun is given in references [2,3,5,8]. The physical implementation of the quadrupoles Q1, Q2, and Q3 is in the form of *wafer-lens* as illustrated later (figures 11-17). The quadrupole MSE lens, Q4 is illustrated in figure 1c, and is a Type II Klemperer lens. The action of the lens in the vertical plane and horizontal plane is shown in figures 3a, 3b respectively. These fields were calculated using a three-dimensional cylindrical coordinate mesh. Most of the development work to determine the shape of the contoured inner electrode displayed in figure 1c, was accomplished using the Type I, In-line Klemperer lens.

Analysis of the Type I Lens

The field problem posed by the In-line lens corresponds to the classic solution of Laplace's equation in a cylindrical cavity with specified boundary values. The potential is given by the Fourier-Bessel expansion:

**Janko B, U.S. Pat. No. 4,188,563, Feb. 1980; Cathode-ray tube having an electron lens system including a meshless-scan-expansion post-deflection accelerating lens.*

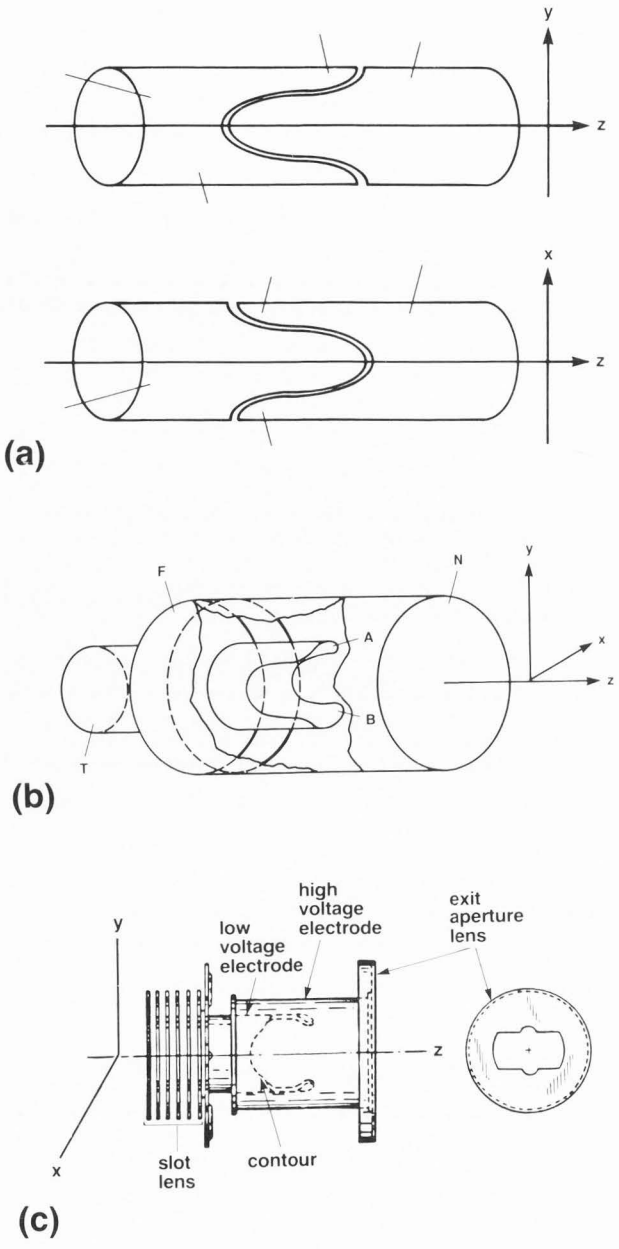

Figure 1. a) Type I Klemperer lens (in line). b) Type II Klemperer lens (LVMSE). c) Accelerating quadrupole Type II lens as used in the Tektronix quadrupole CRT. (Note slot and exit aperture lenses.)

$$V(r,\theta,z) = \sum_{k=0}^{\infty}\sum_{m=0}^{\infty} C_{mk}\, I_{2m}(\hat{k}r)\cos(2m\theta)\cos(\hat{k}z) \tag{1}$$

where for convenience we reflect the structure in figure 1a, about its exit plane $z = L/2$, and assume the symmetry conditions:

$$V(\theta,L - z) = V(\theta,z) = V(\pi - \theta,z). \tag{2}$$

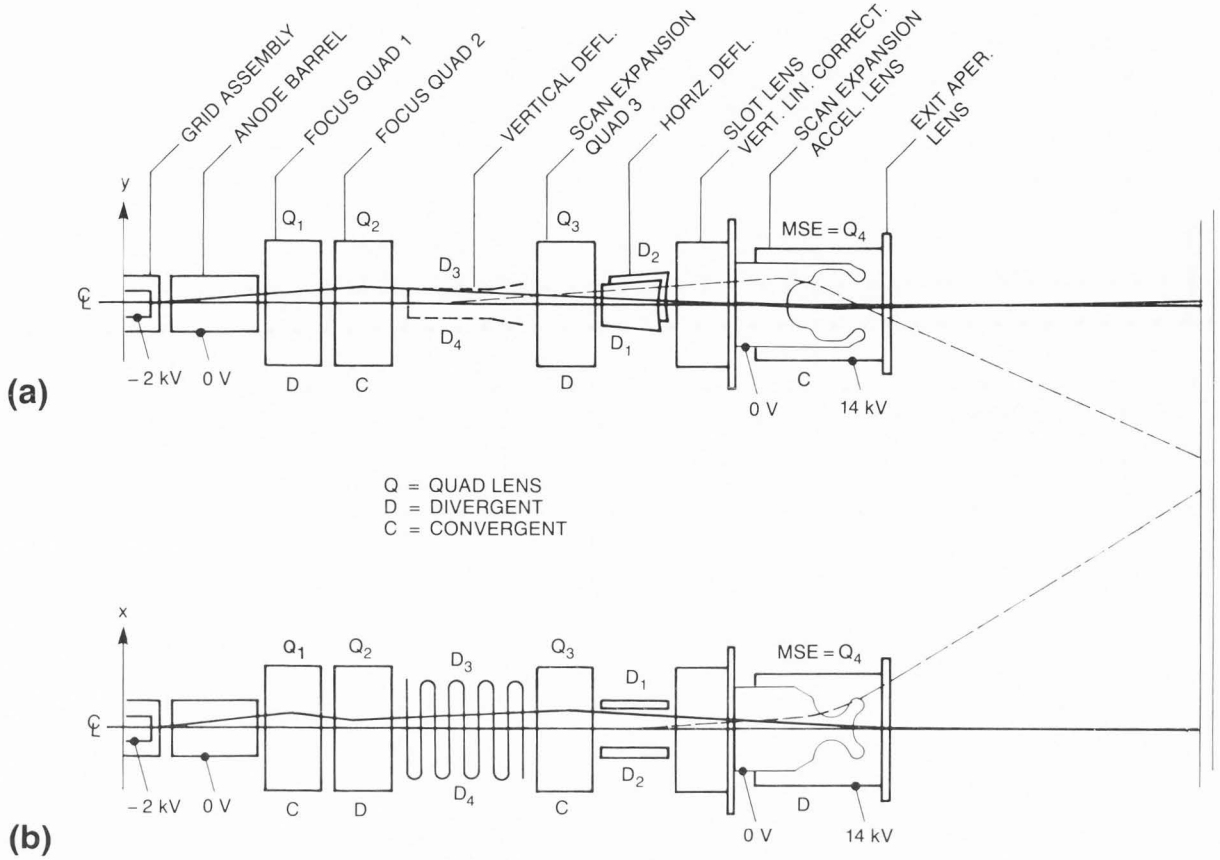

Figure 2. a) Side view of the quadrupole CRT showing the gun's vertical plane of symmetry. b) Top view of the quadrupole CRT showing the horizontal plane of symmetry.

Also $\hat{k} = (2\pi/L)\,k$, and $I_{2m}(\hat{k}r)$ is to be interpreted as the Modified Bessel function of order 2m when $k \neq 0$, and r^{2m} otherwise. The Fourier coefficients C_{mk} are then given by the surface integrals:

$$C_{mk} = \frac{1}{N_{mk}} \iint V(\theta,z)\cos(2m\theta)\cos(\hat{k}z)\,d\theta dz, \tag{3}$$

where $N_{mk} = 4\pi^2 I_{2m}(\hat{k}R)$, $k \neq 0$ (see reference[7]).

Clearly the practical difficulty is to efficiently evaluate these surface integrals for a general class of contours on the surface of the cylinder. What shape of electrodes will be required to eliminate geometry distortion and provide good linearity of the display is generally unknown at the outset. For example, a sinusoid scribed on the surface of the cylinder as a lens shape, yielded a very pincushioned display. The family of curves on the cylinder that has proven to be convenient to work with is made up of concatenations of straight line segments tangent to segments of circular arcs. Such a typical curve is shown in figure 4. A member of this family of curves is described by a list of triads (A,D,R), where A is the angle a line segment of length D makes with the axis of the cylinder (Z-axis), and R is the radius of the circular segment to which it is tangent. These curves have continuous first derivatives and are easy to use.

Evaluating the C_{mk} by Contour Integration

Referring to figure 5a, one quadrant of the surface of a cylinder is divided into 3 regions using contours C_1 and C_2. These regions are assigned voltages V_1, V_2, and V_3 respectively. It is clear that by using Green's Theorem in the plane, the surface integrals (3) can be reduced to contour integrals of the form:

$$M^i_{mk} = \frac{2}{\hat{k}R} \int_{C_i} \sin(\hat{k}z)\cos(2\hat{m}y)\,\frac{dy}{ds}\,ds \quad i = 1,2 \tag{4}$$

where $y = R\theta$, $\hat{m} = m/R$ and $k \neq 0$. The special case $k = 0$ is treated similarly. This results in:

$$C_{mk} = \frac{1}{N_{mk}} \left[(V_1 - V_2)\,M^1_{mk} + (V_2 - V_3)\,M^2_{mk} \right]. \tag{5}$$

The only contribution to the integrals is along C_1 and C_2. These integrations can be performed efficiently by the computer for this general family of contours.

An independent feature on the profile is needed to control horizontal linearity. The four lobes on the profile shown in figure 2 function in this capacity. That the vertical scan crosses through the axis in this plane is most advantageous.

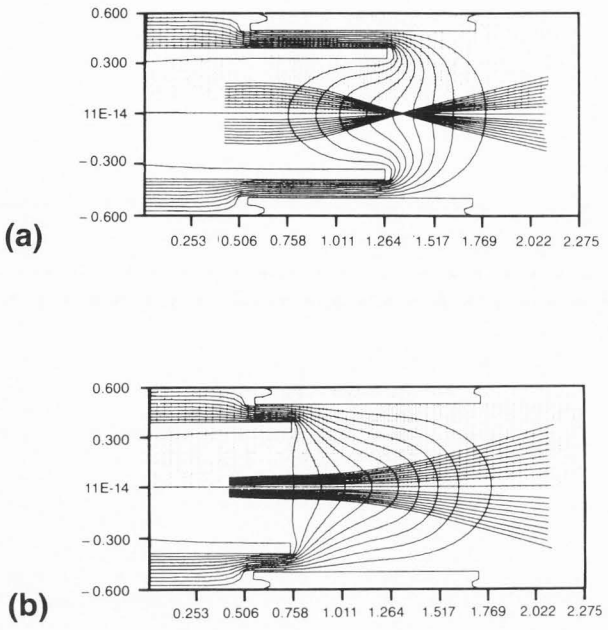

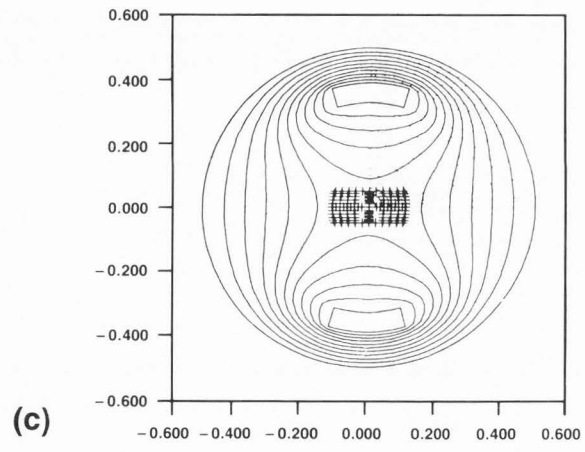

Figure 3. a) Vertical section of a Type II Klemperer lens showing equipotentials and a family of trajectories in the YZ-plane. The exit aperture lens is not included in the calculation. b) Horizontal section of the same lens showing the typical quadrupole characteristic. c) A cross section normal to the Z-axis showing development of the scan. When followed to the CRT face, this scan results in the display shown in Figure 8.

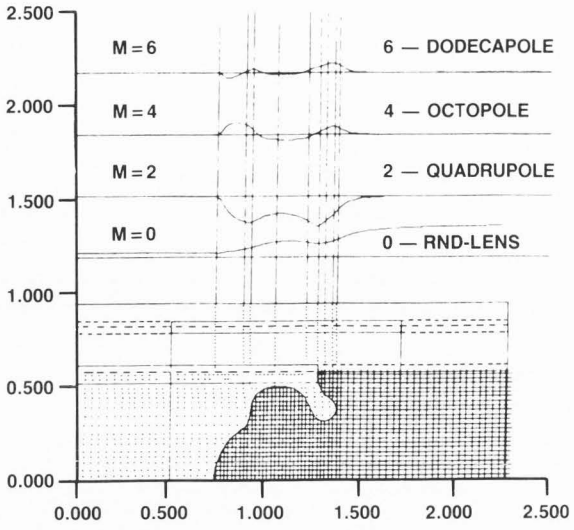

Figure 4. Computer graphics showing the contoured inner electrode, relaxation mesh, and moment functions up to cos(6θ).

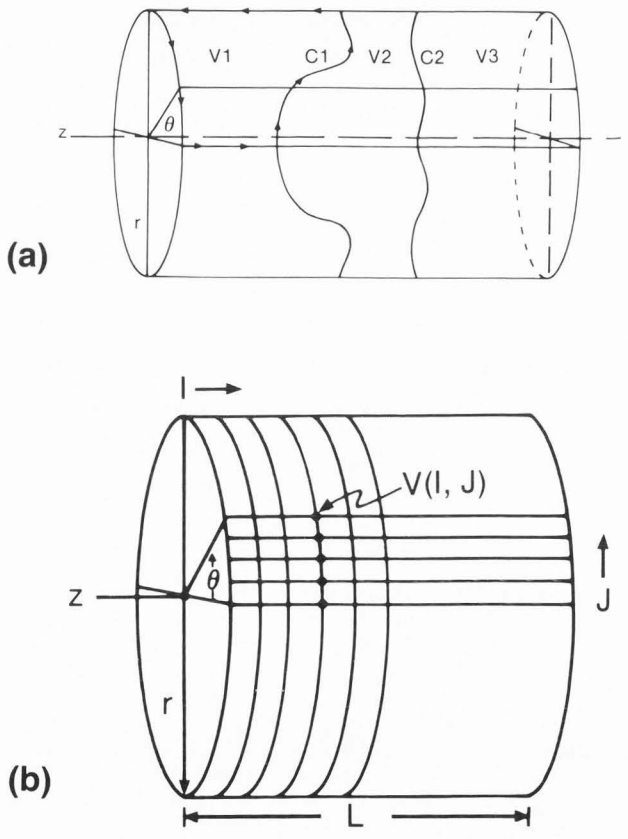

Figure 5. a) Cylindrical surface divided into regions V1, V2 and V3 by contours C1 and C2. A typical contour path of integration, indicated by the arrows, is used to calculate Fourier coefficients. b) Discrete potentials V(I,J) are passed to Fast Fourier Transforms to produce Fourier coefficients.

Evaluating C_{mk} with Fast-Fourier Transforms

A second method of evaluating the C_{mk} that can be used in combination with relaxation methods has proved to be very useful. If $V(z,\theta)$ denotes the boundary potentials on the cylinder, then:

$$A_m(z) = \int V(z,\theta)\cos(m\theta)\,d\theta \qquad (6)$$

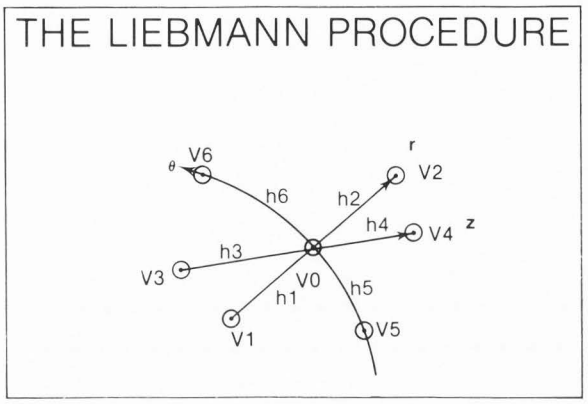

Figure 6. Relaxation formula (8) is applied to a cylindrical mesh. The central node 0 is surrounded by six nearest neighbors 1,2-6 in the r, θ, z coordinate mesh.

is the m-th Moment Function. The Fourier coefficients are then:

$$C_{mk} = \frac{1}{N_{mk}} \int A_{2m}(z) \cos(\hat{k}z)\, dz. \qquad (7)$$

Let the continuous boundary values V(z,θ) be approximated by the discrete values V(I,J), as indicated in figure 5b. For each fixed z_i, the integrals (6) may be evaluated by a call to a Fast-Fourier Transform. After building the discrete functions $A_m(i)$, they are used to evaluate the integrals (7), by further calls to an FFT, for each m. This process for an array of size 100×50, requires about 1 CPU second on a CYBER 170/760.

As indicated above, if the potentials V(I,J), have been determined by any method, relaxation for instance, then the potentials and gradient of the field inside this radius can be determined by evaluating the Fourier series, or respectively, the differentiated series.

Figure 4 illustrates a typical lens profile of Type II, together with the moment functions $A_m(z)$, for $m = 0,2,4,6$. It can be shown that even the multipole corresponding to $m = 8$ has a small but detectable effect on the display.

Analysis of Klemperer Lenses of Type II

It is obvious that the Fourier methods alone will not suffice to determine the fields in the Type II lens. The method employed is relaxation in a three-dimensional cylindrical mesh, the potential matrix V(I,J,K) representing one quadrant of the field. A typical potential matrix may be of dimension V(88,25,35), or 77,000 mesh points. The method depends very heavily on having the electrodes lie in coordinate surfaces. The relaxation process proceeds along coordinate cylinders beginning at the center axis. Boundary analysis also follows the same sequence. The computer graph displayed in figure 4 shows that the mesh density can be varied along each axis as most convenient. The crosshatch shows the mesh distribution as well as giving a convincing demonstration that the program has determined the appropriate relaxation weights. This diagnostic plot shows that for each point sufficiently near the contour, the program has calculated the correct displacements required to perform the relaxation at this point.

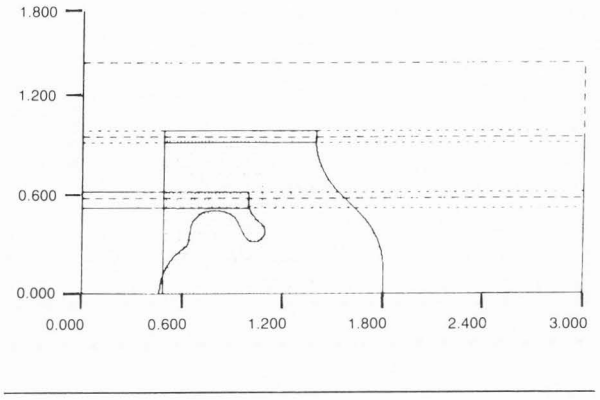

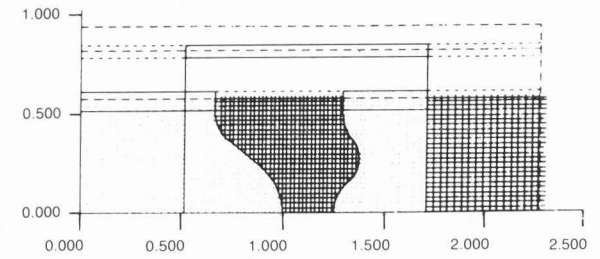

Figure 7. Computer graphics showing software package flexibility. Crosshatch diagnostic shows correct boundary analysis and requires only one CPU second of computer time.

Using the notation indicated in figure 6, the relaxation formula in use becomes:

$$V_0 = \frac{\sum_{i=1}^{6} w_i V_i}{\sum_{i=1}^{6} w_i} \qquad (8)$$

where the weights, $w_1, w_2, \ldots w_6$, are given by:

$$w_1 = \frac{1}{h_1(h_1+h_2)}(1 - h_2/2r) \qquad ,(r \neq 0)$$

(r)

$$w_2 = \frac{1}{h_2(h_1+h_2)}(1 - h_1/2r) \qquad ,(r \neq 0)$$

$$w_3 = \frac{1}{h_3(h_3+h_4)}$$

(z)

$$w_4 = \frac{1}{h_4(h_3+h_4)}$$

$$w_5 = \frac{1}{h_5(h_5+h_6)}$$

(θ)

$$w_6 = \frac{1}{h_6(h_5+h_6)}$$

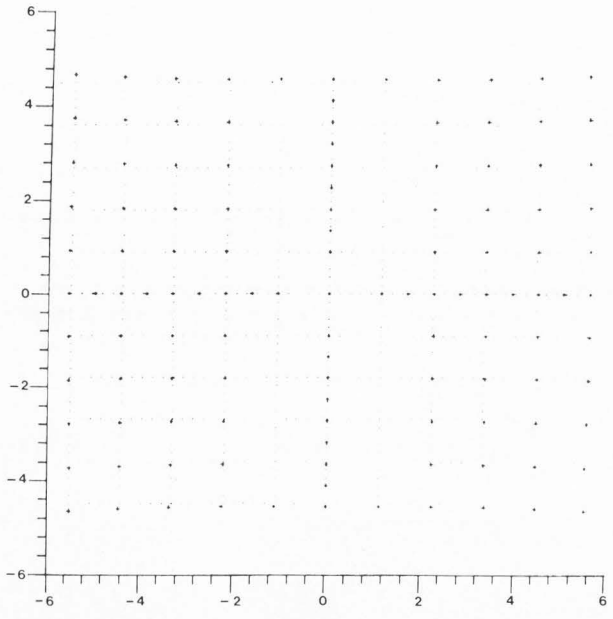

Figure 8. Calculated raster (small +) overlayed by an *ideal* raster (small dot array) is employed to determine lens distortions in the MSE lens. Some pincushion distortion is evident since the exit aperture effect was not included in the calculation.

A modified formula must be used when r = 0. Southwell[17] provides the classic reference for relaxation methods in two dimensions.

The process of determining the displacements h_1, h_2, ... h_6, is the heart of the computer program and has been fully automated requiring no operator intervention. This fact is responsible for the great ease of calculating fields using this technique.

Analysis of Boundary Conditions

Once contours C_1 and C_2 (see figure 5a) have been defined and the mesh distribution specified, the program builds electrode *templates*. A template is an array, NCODE(I,J), containing coded information pertaining to the mesh points which lie in the mesh cylinders falling within the diameter or an electrode. The coded information instructs the relaxation process denoting whether a given point needs *special* or *regular* relaxation weights and whether it is inside or outside the electrode. The program uses an efficient procedure to decide inside-outside issues, for instance to decide if a given mesh node is in region 1 or not. Use of templates makes it possible to store only small tables of *special* relaxation weights; the next special weight to be required always being the next one in the list. Features that make significant reduction in memory requirements are of fundamental importance in the design of a three-dimensional field program.

As shown in figure 7, shaped electrodes can be formed on two concentric diameters. The boundary analysis procedure is very efficient and requires only 1 CPU second on a CYBER 170/760. The short time required for these calculations makes the SETUP procedure for a lens very interactive and the designer can display numerous diagnostic plots and all internally generated quantities at the graphics terminal. The diagnostic plots in figures 4 and 7 are driven by the same subroutine that drives the relaxation process, thus demonstrating that the procedure is performing correctly.

The SETUP program *primes* the relaxation process so that the only calculation that has to be performed during the relaxation stage is the simple arithmetic in equation (8). Since relaxation may take from 15 minutes to an hour of CPU time on a CYBER 170/760, the relaxation process is done in batch mode and not in prime time, to reduce costs. Memory requirements to calculate the Type II lens is 270K octal words, of which 220K words is the large potential matrix. The program is so arranged that during relaxation the potential matrix, the templates and required weight tables are all in high-speed memory together with a minimal amount of FORTRAN code to drive the process. The program does not have to use the disk and hence is not swapped out frequently.

It is expected that if the Fourier series were used to propagate the potentials from the inner electrode surface to the center axis periodically as the relaxation continues, the convergence time could be reduced by 40 to 50 percent. This process has been partially implemented but is as yet untested.

Lens Distortion Analysis

Since the Klemperer lens contains significant multipoles up to cos(8θ), it is clear that 3rd order or even 5th order aberration theory will not suffice to model the geometry distortions of these lenses. The principal method employed to study these distortions is to perform the numerical integration of the equations of motion for a rectilinear family of rays emanating from the deflection centers. Once the deflection centers for the gun are specified, the sequencing of the trajectory calculations to generate the display in figure 8, is fully automated. The rays nearest the center axis on both the X and Y axes are used to define the linear central region from which an *ideal* undistorted raster is generated. In figure 8, the ideal raster is represented by the array of small dots. The calculated raster, determined by the landing positions of the rectilinear family, is then overlaid onto the *ideal* raster. These landing positions are denoted by the heavier crosses. Both geometry and non-linearity distortions can then be seen at a glance. Defocus also can be calculated automatically. This method takes much of the labor out of lens distortion analysis.

The gradients of the field are generated either by a somewhat involved interpolation process in the cylindrical mesh or by employing the Fourier-Bessel series. Since the interpolation near the center axis may not be sufficiently well behaved, the designer can specify a diameter inside of which the program will calculate using the series. Use of the series also allows deeper insight into the effects of various multipoles on the display. Multipoles to be used in the calculation can be specified. Figure 9a shows the dot array resulting from use of only the round-lens and quadrupole terms in the series. When the octopole term is included, the dot array in figure 9b is displayed. This technique together with the moment functions shown in figure 4 provide a way to see what various regions on the profile are contributing to the display.

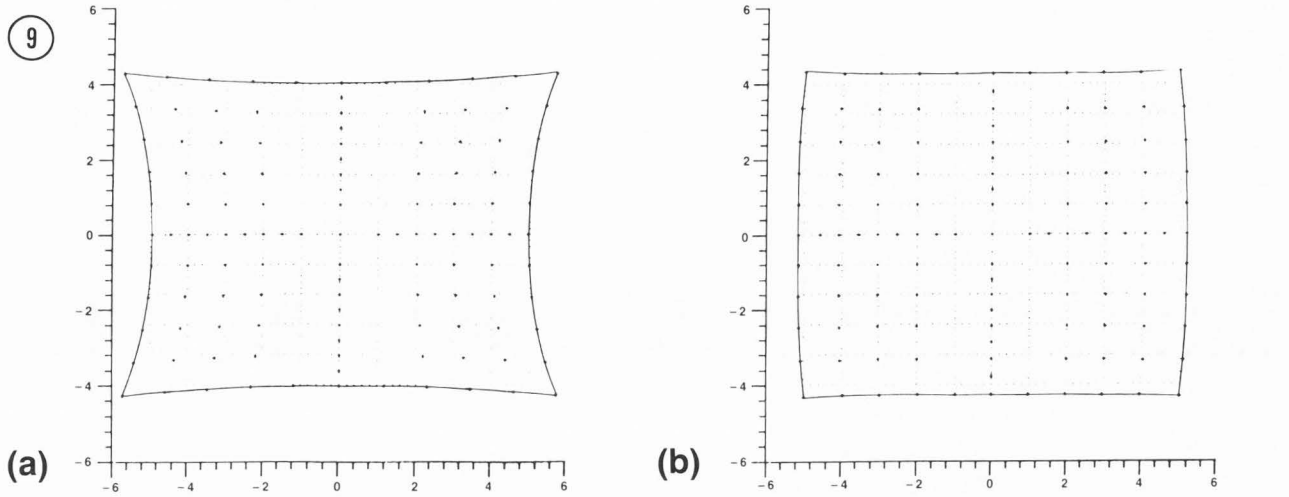

Figure 9. a) Calculated display using only round lens and quadrupole multipoles. b) Calculated display adding the octopole term to the raster calculation.

Lens Performance

Figure 8 shows the quality of the MSE lens field before correction by the exit-aperture lens. The exit-aperture lens shown in figure 1c is a weak lens which removes the residual pincushion in the horizontal lines. This lens was designed empirically. Computer code has been written to model the exit aperture lenses but it remains untested at this time. Figures 8 and 16c illustrate the effect of the *slot-lens* whose function is to correct vertical linearity. Vertical linearity before correction by the slot-lens is shown in figure 10b as a function of the ratio between cathode potential and screen potential. Displayed in figure 10a, calculated focal lengths agree well within the range of experimental error with measured data. See reference [3,5] for details of the MSE quadrupole system performance.

The slot-lens is one example of what is called a *wafer-lens*. The description of a general software package to analyze such structures follows.

Wafer-Lens Analysis

Implementation of quadrupoles Q_1, Q_2, Q_3 and the *slot-lens* in the Quadrupole CRT take the form of sequences of flat wafer electrodes. These wafers contain various apertures with two planes of symmetry. Lenses formed in this manner can be accurately aligned and are inexpensive. Early modeling of quadrupoles was done using the transformations noted by Martin and Deschamps[12], for *ideal* quadrupoles. These quadrupole models have limited usage and cannot be used to study aberrations nor to accurately relate structural dimensions to the required operating voltages. Considerable octopole moment is intentionally introduced into the Q_3 lens to compensate for a defocusing effect in the MSE lens. This defocusing effect cannot be treated by any known approximate model. On the other hand, the action of the slot-lens can be treated approximately by assuming the slots are of infinite extent in the horizontal direction. Field calculation is then reduced to a two-dimensional problem and can be calculated by existing programs. However, the finite width of the slot apertures in the XZ-plane produces significant unwanted lens effects in the horizontal plane. These effects can only be determined by a three-dimensional field program.

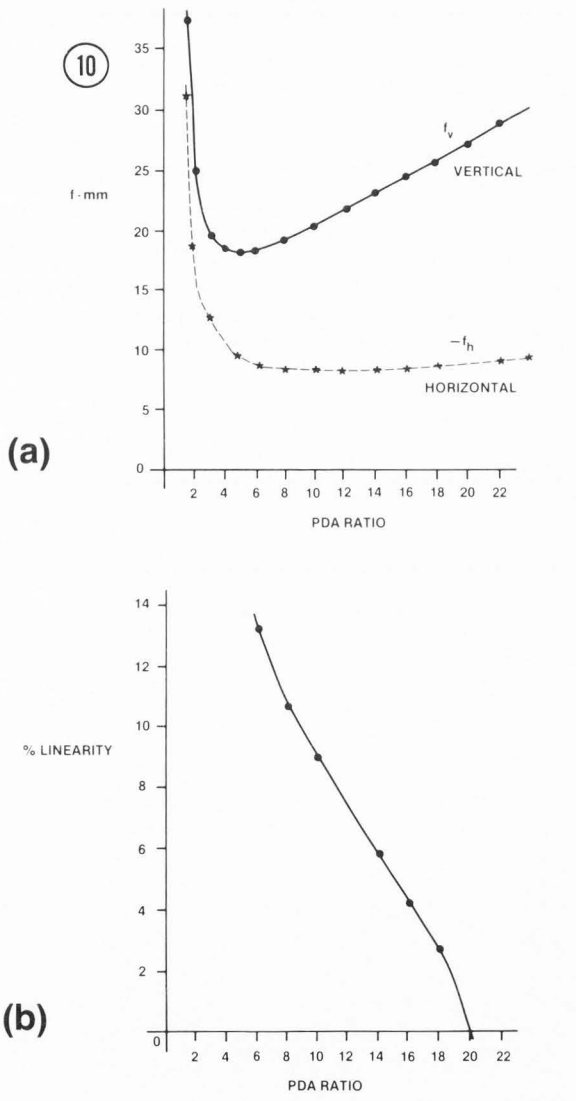

Figure 10. a) Horizontal and vertical focal lengths are shown as a function of PDA ratio (ratio of cathode to screen potential). b) MSE vertical lens non-linearity with slot lens turned off.

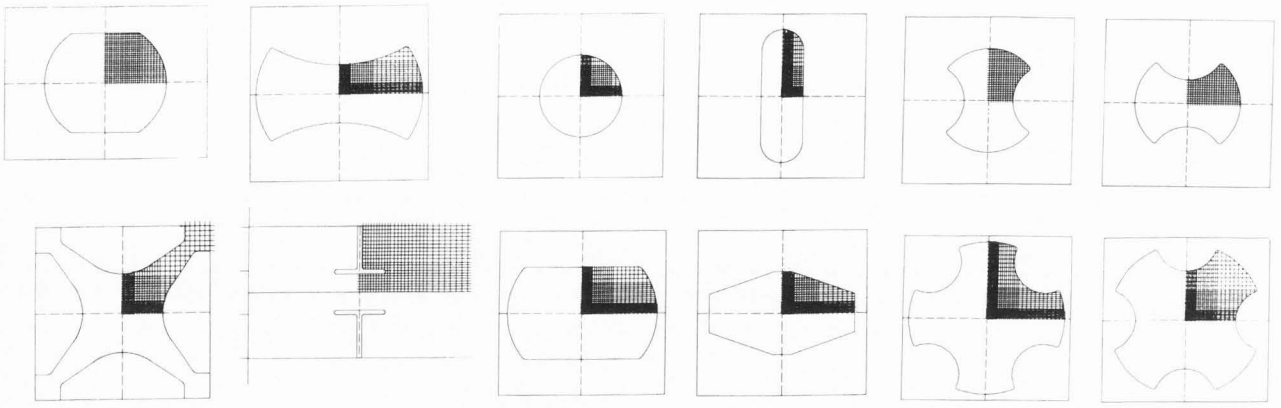

Figure 11. Various aperture types that can be generated with the wafer software program.

After developing a program to study Type II Klemperer lenses, it was realized that the same software techniques could be used to analyze a large class of wafer-lenses. Such a program has been developed at Tektronix and is essentially complete. Typical apertures that can be treated by the program are illustrated in figure 11. These wafer electrodes are not assumed to be thin structures and can even have more than one voltage assigned as in the *solid-quadrupole* discussed below. It is also possible to use the program to study a class of segmented-plate electrostatic deflectors by forcing a ground plane in the XZ-plane. The fringe fields and interaction with the shields can be investigated. This discussion, however, is restricted to three examples: the Q_3 lens shown in figures 12–15, the slot-lens of figure 16, and the *solid-quadrupole* pair of figure 17.

General Program Features

Most of the apertures in figure 11 can be described by three to five parameters. Besides the *general* element, there are 13 aperture types that can be defined very simply by a minimal set of parameters. The *general* element allows the CRT designer to create many complex aperture shapes. These apertures are again formed from concatenations of straight line segments, tangent to segments of circular arcs.

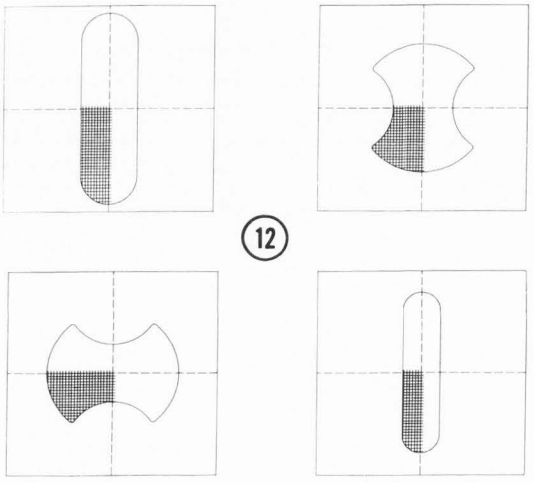

Figure 12. Menu of apertures used in the Q3 lens.

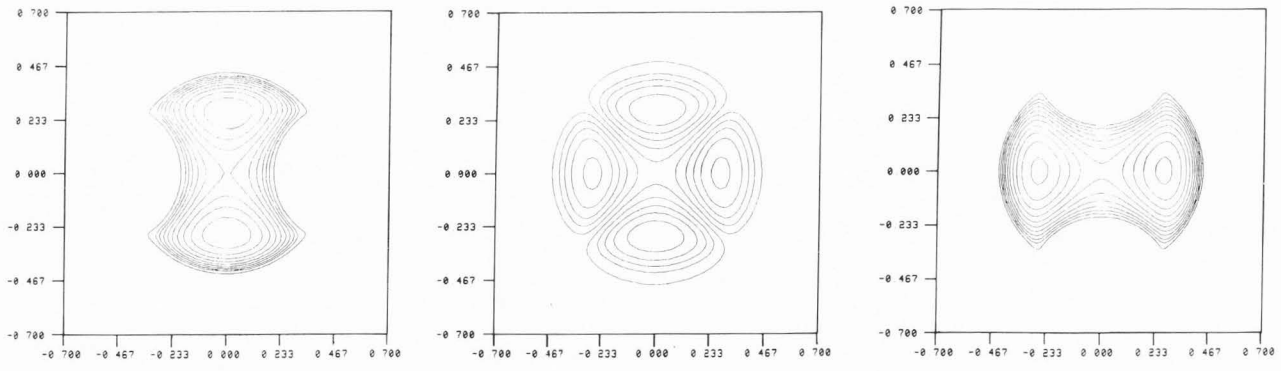

Figure 13. Typical equipotential plots in various cross sections of the Q3 lens. Calculations were performed using relaxation in a Cartesian coordinate mesh.

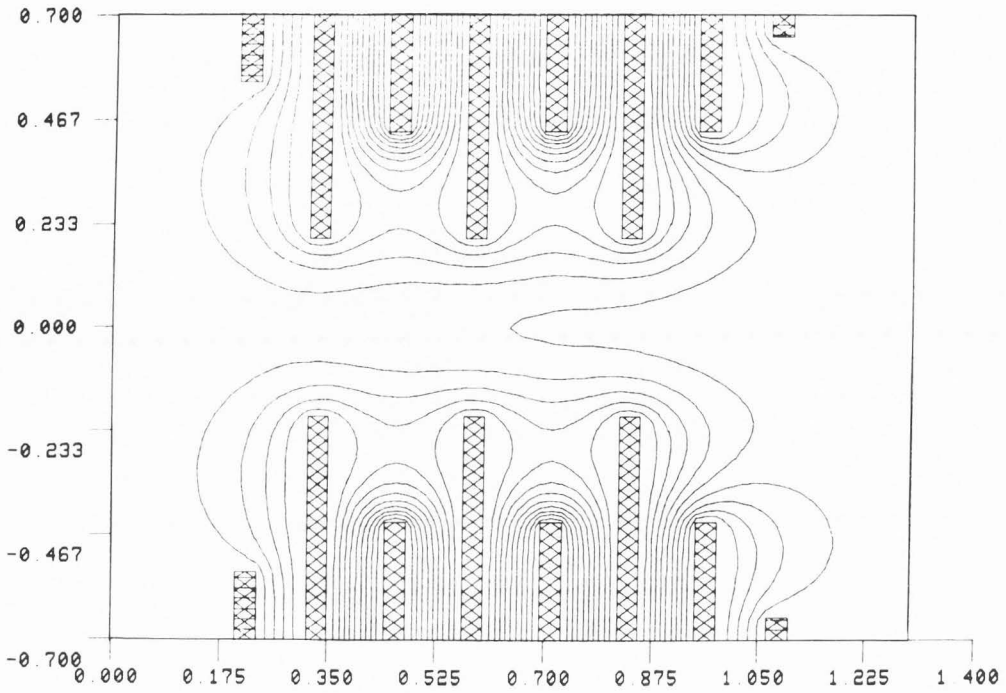

Figure 14. Equipotentials are displayed in a vertical cross section of the Q3 lens.

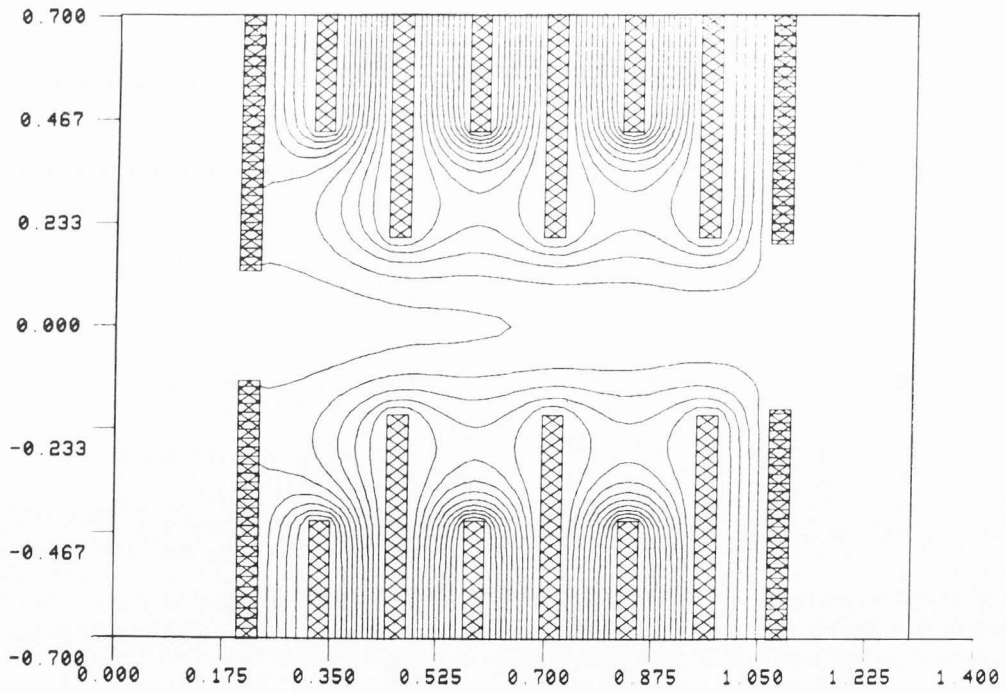

Figure 15. Horizontal cross section of the Q3 lens displaying equipotentials.

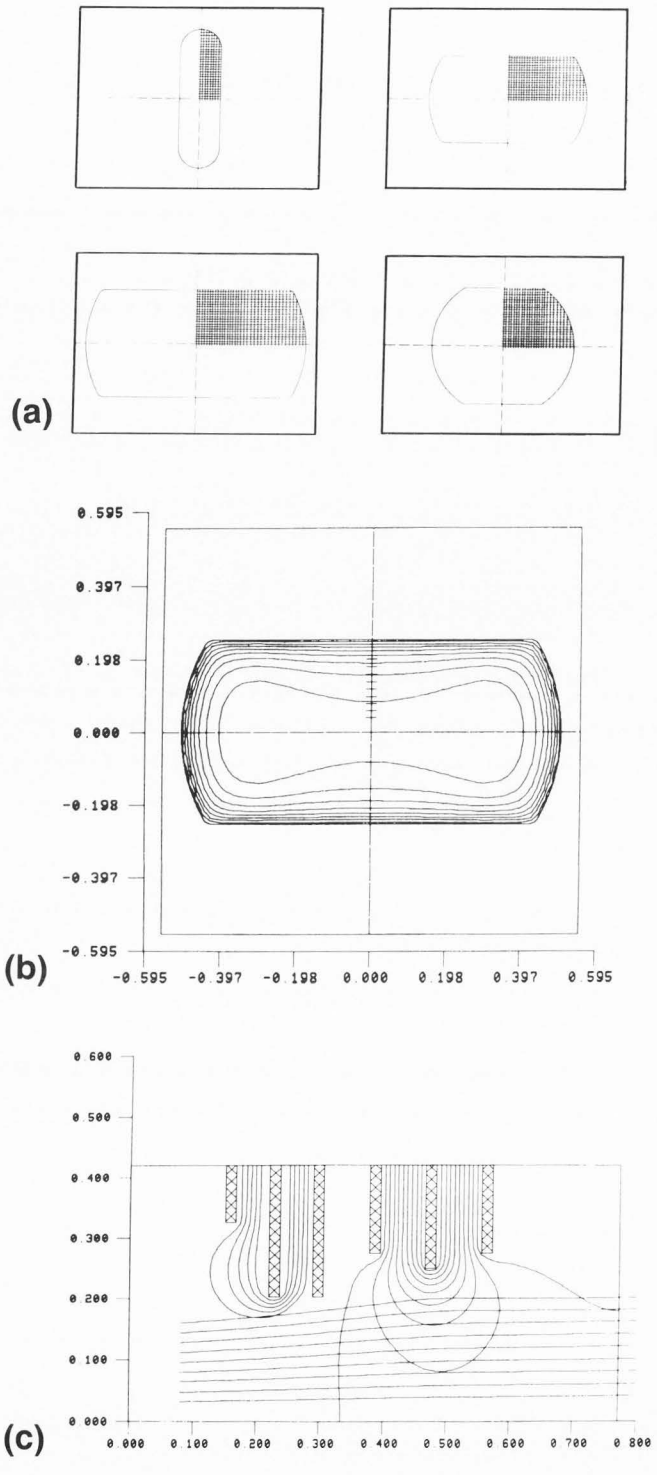

Figure 16. a) Menu of apertures for the slot lens. b) Equipotentials in the plane of the slot wafer (second from right in 16c). Crosses show where the trajectories pierce the plane. c) Vertical cross section of the slot lens showing the action of the field on the vertical scan as it passes the slot wafer.

Three special elements exist: vacuum space, Neumann boundary, and a voltage plane. For a given problem the designer defines a *menu* of apertures from which elements can be selected to form a lens system. The lens configuration is defined simply by specifying a sequence of indices which point to the desired member of the *menu*. The same aperture can be used repeatedly with different voltages. For each element, thickness, voltages and number of Z-planes is specified. This information essentially defines a lens configuration. Once the XY-mesh spacing has been given the program analyzes boundary conditions and computes all the required relaxation weights. This happens automatically without operator intervention and provides many diagnostic plots, if desired. The designer might for instance wish to insert an octopole element into a quadrupole to compensate for unwanted spot distortions in the system.

The Q3 Lens

Figure 12 shows the *menu* of apertures used for the Q3 lens. This example is actually a two times scale up of the lens used in the quadrupole MSE gun. Figure 13 displays the equipotential contours in typical apertures and in a plane midway between them. Figures 14 and 15, respectively, illustrate the YZ and XZ cross-sections of the Q_3 lens. Fields are calculated by relaxation in a three-dimensional, Cartesian coordinate mesh. It was somewhat surprising to find that the relaxation process converged in approximately 1/5 to 1/7 the time for the typical MSE lens field calculations. The relaxation time for the Q_3 lens was 359 CPU seconds on a CYBER 170/760. One quadrant of the field was represented by a matrix of size V(35,35,77). The maximum residual dropped to 0.00005 volts in 121 iterations through the matrix.

Useful Techniques

The Schwarz-Alternating-Procedure (SAP)[16] can be very useful for solving complex boundary value problems. A form of this procedure is used at Tektronix to calculate the fields in *wafer-lenses*. Slightly more than half of the total field is kept in the high speed memory of the computer at any given time. The remainder resides on the disk. A communicating overlap region is mapped back and forth in memory as the two segments of the field are swapped in and out of high speed memory. For the Q_3 lens, for instance, the total field had 77 Z-planes. Segment 1 contained 45 Z-planes. The overlap region consisted of 13 Z-planes. Hence segment two also contained $(77-45)+13=45$ mesh planes. Each segment was relaxed five times before being swapped out again. The overlap region is relaxed twice as often as the rest of the field.

Voltage Scaling

Voltage scaling has been an often used procedure. In calculating three-dimensional fields this process becomes imperative since the relaxation times are fairly long. At this time the Tektronix program is set up to handle voltage scaling for three independent voltages. If two independent solutions of the fields have been calculated, then any other set of voltages can be obtained by linear super-position. Since voltage scaling requires only about one to two CPU seconds on a CYBER 170/760, interactive voltage changes can be made on the lens followed by immediate display of the new equipotentials.

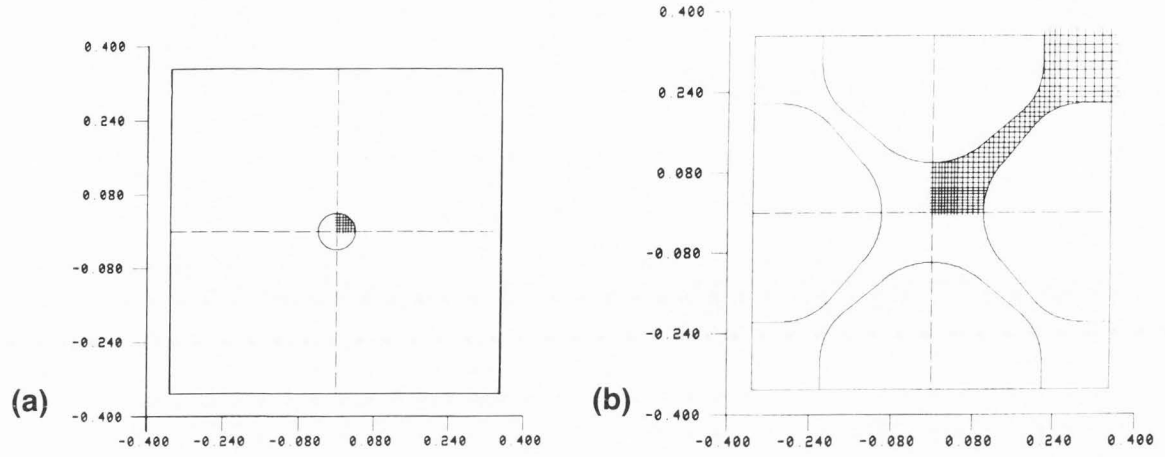

Figure 17. Solid quadrupole pair. a) Isolation shield. b) Wafer cross section. c) Vertical cross section and a pair of trajectories. d) Equipotentials in cross section of the lens.

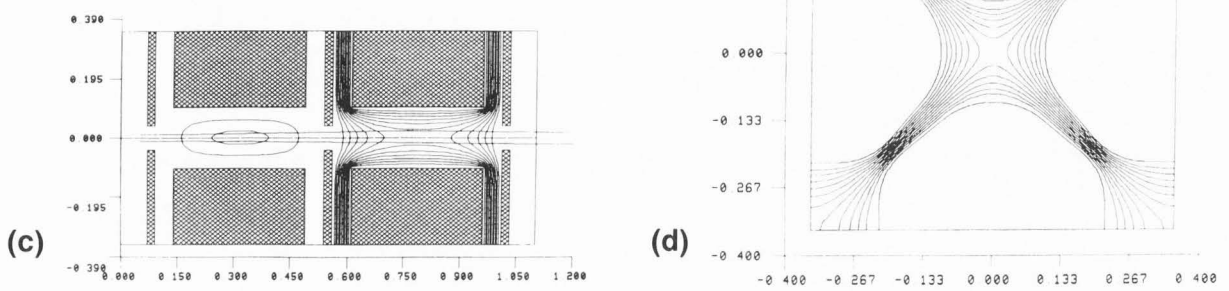

Initializing With Old Potentials

Calculation times can drop to about one third by initializing the relaxation using the potentials from a similar investigation. This is generally the case if the geometry of the lens has changed only slightly or a spacing has changed. If the lens design is progressing incrementally, calculations can be fairly inexpensive.

The Slot Lens

In figure 16c the wafer second to the last is called the *slot* wafer. It operates at a potential of about 1 kV below its neighbors. Non-linear distribution of the equipotentials near the wafer are shown in two aspects in figures 16b and 16c. The primary effect of the lens is to change the slope of the rays in the vertical scan as they pass the slot wafer. The net result is to improve the vertical linearity of the system. The program can display graphically the positions of trajectories as they penetrate any Z-plane (see figure 16b). For this illustration the slot field was represented by a potential matrix of size V(40,35,76) and was constructed with field segments of length 45 and 44, and an overlap of 13 planes. The relaxation process required 17.5 minutes of CPU time on the CYBER to reduce the maximum residual to 0.00013 volts. A total of 500 passes through the matrix was required.

A Solid Quadrupole Pair

Figure 17 is an example using *thick* electrodes which also employ two voltages for a single element. Two trajectories are displayed in figure 17c. This field was calculated using a potential matrix of size V(35,35,79). Both field segments were of length 45 and an overlap region consisting of 11 Z-planes. Total iterations was 90 to bring the maximum residual down to 0.00003 volts. 233 CPU seconds were required for the calculations.

Conclusions

For the class of lenses discussed herein the developmental setup effort by any other known method would be very labourious, if possible at all. On the other hand, some of the examples above can be setup in less than one hour using the software programs and techniques presented here. The software methods used in the analysis of wafer-lenses could be extended to allow for non-symmetric apertures or wafer displacements normal to the Z-axis. Clearly, all four quadrants of the fields would have to be represented and relaxation times would be quite long. Misalignments of the MSE structures could best be handled by the Boundary Element Method. It may well be possible to automate setting up the BEM procedure for a broad class of structures. The

BEM method could more easily handle general *tilts* and misalignments. Application of the Fast Fourier Transform can be easily used to decompose the central field into its multipole moments, thus giving more insight into the fields.

References

[1] Coons SA, (1974) "Surface patches and B-spline curves in computer aided geometric design," Barnhill and Riesenfeld, Eds. *Academic Press.*

[2] Franzen N, (1983) "A quadrupole scan expansion accelerating lens system for oscilloscopes," *Society for Information Display Technical Digest,* Vol. 14, pp. 120–121, *Lewis Winner,* Coral Gables, Florida.

[3] Franzen N and Janko B, (1983) "Meshless scan expansion CRT improves trace quality," *Electronic Imaging,* Vol. 2–7, pp. 48–53, *Morgan-Grampian,* Boston Mass.

[4] Harrington R, (1967) "Matrix methods for field problems," *Proc. of IEEE,* Vol. 55, No. 2, pp. 136–149.

[5] Hawken K, Franzen N and Sonneborn J, (1983) "A novel high-performance CRT with meshless scan expansion," *Proc. of 3rd International Display Research Conf.,* Kobe Japan, pp. 136–139.

[6] Hosokoshi K, Ashizaki S and Suzuki H, (1983) "Improved OLF in-line gun system," *Proc. of 3rd International Display Research Conf.,* Kobe Japan, pp. 272–275.

[7] Jackson D, (1975) Classical Electrodynamics, 2nd Ed., *Wiley,* pp. 102.

[8] Janko B, Franzen N, Sonneborn J, (1983) "CRT architecture with meshless scan expansion," *Society for Information Display Digest,* Vol. 14, pp. 118–119, *Lewis Winner,* Coral Gables, Florida.

[9] Klemperer O, (1953) Electron Optics, pp.297–298, *Cambridge Univ. Press.,* 2nd Ed.

[10] Lean M and Wexler A, (1982) "Accurate field computation with the boundary element method," *IEEE Trans. on Mag,* Vol. MAG-18, pp. 331-335.

[11] MacGregor DM, (1983) "Computer-aided design of color picture tubes with a three-dimensional model,"*IEEE Conf. Proceedings of International Conference on Consumer Electronics,* Des Plaines, Ill., pp.130.

[12] Martin A and Deschamps J, (1971) "A short-length rectangular oscilloscope tube with high deflection sensitivity by an original technique," *Proc. Society for Information Display,* Vol. 12/1, pp. 16–21.

[13] Munro E and Chu HC, (1982) "Numerical analysis of electron beam lithography systems," Part I, *Optik 60, No. 4* and Part II, *Optik 61, No. 1, Wissenschaftliche Verlagsgesellshaft mbH,* Stuttgart.

[14] Odenthal C, (1977) "A box-shaped scan-expansion lens for an oscilloscope CRT," *Society for Information Display Digest,* Lewis Winner, NY, pp. 134–135.

[15] Ritz E, (1979) "Recent Advances in Electron Beam Deflection," *Advances in Electronics and Electron Physics,* Vol. 49, *Academic Press,* pp. 299-356.

[16] Schaefer C, (1983) "The application of the alternating procedure, by H.A. Schwarz, for computing three-dimensional electrostatic fields in electron-optical devices with complicated boundaries," *Optik 65,* No. 4, pp. 347-359.

[17] Southwell R, (1940) Relaxation Methods in Engineering Science, *Oxford U. Press.*

[18] Yildir Y and Wexler A, (1983) "MANDEP-A FEM/BEM data preparation package," *IEEE Trans. on Magnetics,* Vol. MAG-19, No. 6, pp.2562.

Acknowledgement

The author wishes to give special thanks to Doctor Friedrich Lenz, Professor, University of Tubingen, West Germany, for the excellent courses in Electron Optics which he delivered at Tektronix over the years. His presence is always a great inspiration. Many thanks also to the members of the Display Device Engineering Group at Tektronix for their support of this work.